Revision 1

Formation of SiH_4 and H_2O by the dissolution of quartz in H_2 fluid under high pressure and temperature

Ayako Shinozaki[a], Hiroyuki Kagi[a], Naoki Noguchi[a*], Hisako Hirai[b], Hiroaki Ohfuji[b], Taku Okada[c], Satoshi Nakano[d], and Takehiko Yagi[b]

[a] Geochemical Research Center, Graduate School of Science, The University of Tokyo, Hongo, Tokyo 113-0033, Japan

[b] Geodynamics Research Center, Ehime University, 2-5 Bunkyo-cho, Matsuyama, Ehime, 790-8577, Japan

[c] Institute for Solid State Physics, The University of Tokyo, Kashiwanoha, Kashiwa, Chiba 277-8581, Japan

[d] National Institute for Materials Science, Namiki, Tsukuba, Ibaraki 305-0044

14 Corresponding author: Ayako Shinozaki

15 Phone number: +81-3-5841-4450

16 E-mail address: shinozaki@eqchem.s.u-tokyo.ac.jp

17 Full postal address: 7-3-1 Hongo, Bunkyo-ku, Tokyo 113-0033, Japan

18

19 *Present address: Department of Applied Chemistry, Graduate School of Engineering,

20 Hiroshima University, Hiroshima, 739-8527, Japan

21

Abstract

Species dissolved in H_2 fluid were investigated in a SiO_2–H_2 system. Raman and infrared (IR) spectra were measured at high pressure and room temperature after heating experiments conducted at two pressure and temperature conditions: 2.0 GPa, 1700 K and 3.0 GPa, 1500 K. With the dissolution of quartz, a SiH vibration mode assignable to SiH_4 was detected from Raman spectra of the fluid phase. Furthermore, an OH vibration mode was observed at 3260 cm^{-1} from the IR spectra at 3.0 GPa. With decreasing pressure, the OH vibration frequencies observed between 3.0 GPa and 2.1 GPa correspond to that of ice VII, and those observed at 1.4 GPa and 1.1 GPa correspond to that of ice VI. These results indicate that the chemical reaction between dissolved SiO_2 components and H_2 fluid caused the formation of H_2O and SiH_4, which was contrastive to that observed in SiO_2–H_2O fluid. Results imply that a part of H_2 is oxidized to form H_2O when SiO_2 components of mantle minerals dissolve in H_2 fluid, even in an iron-free system.

Key words: H_2–H_2O fluid; dissolution; Raman; IR; laser-heated diamond anvil cell

Introduction

Fluids in the Earth's mantle influence phase relations, melting temperatures, chemical compositions, and physical properties of co-existing silicate minerals. Consequently, fluids in the mantle play an important role in elemental transportation, melt formation, and mantle dynamics. Stability and phase relations of silicate minerals depend on the Mg/Si ratio of silicate components dissolved in the coexisting fluid. For example, the silicate composition dissolving in H_2O fluid changes sharply from SiO_2-rich to MgO-rich around 3 GPa, providing a change of the thermodynamically stable phase in $MgSiO_3$-H_2O system from enstatite+forsterite+fluid to enstatite+fluid (e.g. Zhang and Frantz 2000; Stalder et al. 2001; Mibe et al. 2002; Kawamoto et al. 2004). Such a change of Mg/Si ratio is regarded as induced by a change of the dissolution species of silicate components in H_2O fluid. The dissolution of silica in H_2O fluids has been extensively studied over a wide range of pressures and temperatures; the silica species observed in H_2O fluids are SiOH groups such as H_4SiO_4 and $H_6Si_2O_7$ below 3 GPa (e.g. Anderson and Burnham, 1965; Manning, 1994; Shen and Keppler, 1995; Zotov and Keppler, 2000; Zotov and Keppler, 2002; Newton and Manning, 2003; Newton and Manning, 2008; Mysen, 2009; Mysen, 2010). At pressures higher than 3

GPa, the existence of MgOH groups was reported from an investigation of the hydrous silicate melt structure (Yamada et al., 2011).

Fluids in the Earth's mantle contain considerable amounts of H_2 in addition to H_2O. The ratio of H_2/H_2O is likely to depend on the surrounding oxidation state. In general, the crust and the shallow mantle are in an oxidizing condition (close to FMQ buffer) (Frost and McCammon, 2008). Consequently, fluids in the shallow depth contain little H_2. The mantle is reduced progressively with depth. Then the oxidation state becomes close to the iron–wustite buffer at depths greater than >200 km (e.g. Woodland and Koch, 2003; McCammon and Kopylova, 2004; Rohrbach et al., 2007; Frost and McCammon, 2008; Goncharov et al., 2012). Thermodynamical calculations demonstrated that a molar fraction of H_2 is expected to increase concomitantly with increasing depth and approached about 10–20% in such reduced mantle (e.g. Ballhaus, 1995; Frost and McCammon, 2008; Goncharov et al., 2012). Moreover, Sokol et al. (2009) demonstrated experimentally that the molar fraction of H_2 becomes >50% at 6.3 GPa, 1873 K, in the iron–wustite buffer. Results of these studies show that H_2 is a major component of fluids in the reduced mantle.

The existence of H_2 is predicted even in the shallow mantle because the oxygen

fugacity does not vary with depth only, but also with local settings (Wood et al., 1990). For example, a certain amount of H_2 is producible by serpentinization in the shallow mantle (Sleep et al., 2004). In addition, H_2 is estimated as a major component in the atmosphere of the early Earth (e.g. Hashimoto et al., 2007; Schaefer and Fegley, 2007). A considerable amount of H_2 can be dissolved in the magma ocean (Hirschmann et al., 2012). In the pressure and temperature conditions of the shallow part of the early mantle, immiscibility between H_2O and H_2 fluid is likely to occur (Bali et al., 2013), implying that H_2 fluid exists even in high purity in such a condition. These studies indicate that H_2 exists even in the shallow mantle both in the present Earth and in the early Earth. Therefore, the influence of H_2 on the phase relations of surrounding silicate minerals should be investigated in a wide range of pressure and temperature conditions, as well as in studies of H_2O and silicate minerals.

For the Mg_2SiO_4-H_2 system, we found recently that forsterite (Mg_2SiO_4) decomposed to form periclase (MgO) with dissolution of SiO_2 components at 2.5–15.0 GPa and around 1500 K (Shinozaki et al., 2013). In addition, the quartz dissolution was observed in a SiO_2-H_2 system, although periclase was dissolved only slightly in a MgO-H_2 system (Shinozaki et al., 2013). The decomposition of forsterite and

crystallization of periclase indicated that the Mg/Si ratio in H_2 fluid is markedly lower than that in H_2O fluid, in which forsterite is stable with H_2O fluid up to around 10 GPa (e.g. Inoue, 1994; Stalder et al., 2001; Mibe et al., 2002; Kawamoto et al., 2004). To reveal the reason for the difference in Mg/Si composition dissolved between H_2 and H_2O fluids, the dissolution species in the fluid phases should be investigated. In this study, species of dissolved component in H_2 fluid were investigated in a SiO_2-H_2 system using Raman and infrared spectroscopy under high pressure.

Material and methods

High-pressure and high-temperature experiments were performed using a diamond anvil cell (DAC) with 450 μm and 600 μm culets. A hole drilled in a rhenium gasket after pre-compression was used as a sample chamber. The sample chamber diameter and the thickness before the experiment were about 200 μm and about 150 μm, respectively. The sample chamber thickness became about 75 μm after the experiment. The starting materials used for this study were natural quartz (SiO_2) and hydrogen gas (H_2; 99.99999% purity). A few particles of quartz crystals with a grain size of about 50–150 μm were polished to about 50 μm thickness from both sides and were then loaded into a sample chamber together with ruby particles. Then, H_2 gas was introduced into a

sample chamber as a supercritical fluid after compression at approximately 0.13–0.18 GPa at room temperature using gas-loading apparatuses (Yagi et al., 1996; Takemura et al., 2001). Pressure was measured using the ruby fluorescence method (Mao et al., 1978).

Samples were first compressed to the target pressure at room temperature and were then heated from a single side using a CO_2 laser. Temperature was measured using spectroradiometry. The uncertainty of the heating temperature was estimated as ± 200 K from the lateral temperature distribution in the sample chamber and the fluctuation of laser power. The heating duration was about 5–10 min. The samples were quenched to room temperature by turning off the laser. In this study, two runs were performed, respectively, at 2.0 GPa and 1700 K, and 3.0 GPa and 1500 K.

Raman spectra of the samples were observed using micro-Raman spectrometry under high pressure and room temperature. The typical constitution of a Raman spectrometer is the following: an Ar^+ laser (λ=514.5 nm) (about 10 mW at the sample surface), an optical microscope with objective lens (typically 20× magnification and 0.35 numerical aperture), single polychromator, and CCD-detector. Scattered light was dispersed using a grating with 1200 grooves per millimeter. Raman bands of naphthalene, silicon, and neon emission lines were used for Raman shift calibration. The spectral

resolution was approximately 2 cm^{-1}. The typical accumulation time for each measurement was approximately 60 s. IR absorption spectra were obtained at BL43IR in SPring-8 at high pressure and room temperature with synchrotron radiation as a light source, an FT-IR spectrometer (Hyperion2000; Bruker Co.), a Ge-coated KBr beam splitter, and an InSb detector. All measurements were performed in transmission mode. The aperture was 15 μm ×15 μm. The wavenumber resolution was set to 4 cm^{-1}.

3. Results

Figure 1a and Figure 1b show representative Raman spectra obtained from the sample in DAC before and after heating. Before heating, the Raman spectrum was obtained from the area which both a quartz grain and H_2 fluid existed. The observed frequencies of SiO vibration modes of quartz and vibration modes of H_2 molecules correspond to those of quartz (Dean et al., 1982; Schmidt and Ziemann, 2000) and pure H_2 fluid (Sharma et al., 1980), respectively. By laser heating at 1700 K and 2.0 GPa, quartz crystals dissolved in H_2 fluid and almost disappeared from the laser heating spot, as described in a previous report (Shinozaki et al., 2013). After heating, the Raman spectra of the fluid phase were measured at the heating spot, where SiO vibration modes of quartz almost disappeared. However, peaks from hydrogen molecules were observed

without marked frequency shifts compared with those obtained before heating (Figs. 1a, 1b). In the surrounding part of the laser heating spot, quartz crystals remained. Coesite, a denser phase of quartz, was not detected from the Raman spectra.

Figure 2a shows representative Raman spectra collected from the heating area from 2100 cm^{-1} to 2300 cm^{-1} with decreasing pressure after heating. A peak assignable to a SiH stretching mode newly appeared at 2228 cm^{-1} at 2.8 GPa. The frequency of the new peak differed markedly from a stretching mode of carbon monoxide, which was observed around 2140 cm^{-1} at around 3 GPa (Katz et al., 1984). The peak height of the SiH vibration mode was approximately <1/17 of that of the H_2 stretching mode. Figure 2b shows the pressure-dependence of the SiH vibration mode frequency. The SiH vibration peak shifted to a lower frequency with decreasing pressure down to 0.4 GPa. The SiH vibration peak disappeared at ambient pressure with the release of H_2 fluid from the sample chamber. The SiH vibration peak was not detected when we measured the unreacted quartz crystals. These results indicate that the SiH group existed not in the quartz crystal structure, but in the fluid phase.

IR spectra were measured at room temperature and high pressure to examine the existence of OH vibration mode after heating at 1500 K and 3.0 GPa (Fig. 3). Figure

158 4a shows representative IR spectra with decreasing pressure, as obtained exclusively
159 from the fluid phase smaller than 30 μm in one direction. High spatial resolution of the
160 FT-IR with synchrotron radiation enabled the measurements, which were done in the
161 measured area depicted in Fig. 3. An OH stretching mode was observed at 3260 cm^{-1} at
162 3.0 GPa. Additionally, weak peaks assignable to the vibration mode of H_2 molecules
163 were observed at 4211 cm^{-1}. Combination modes of the vibration mode plus the rotation
164 mode of molecular H_2 were observed at 4622 cm^{-1} and 4805 cm^{-1} (Fig. 4a) (Gush et al.,
165 1960). Absorbance of the OH vibration mode was about 0.37 at 3.0 GPa. The OH
166 vibration mode shifted to higher frequency with decreasing pressure down to 2.1 GPa
167 (Figs. 4a, 4b). At 1.4 GPa, the OH vibration peak jumped to a lower frequency at 3200
168 cm^{-1}. The peak shifted to higher frequency with decreasing pressure down to 1.1 GPa.
169 Below 0.6 GPa, the OH vibration peak almost disappeared along with vibrations
170 derived from H_2 molecules, indicating the release of the fluid phase from the sample
171 chamber at approximately that pressure.

172 **Discussion**

173 Dissolution of quartz in H_2 fluid was observed after heating in two conditions:
174 2.0 GPa, 1700 K and 3.0 GPa, 1500 K. The SiH vibration and OH vibration modes were

found from the fluid phase measured by Raman and IR spectroscopies. SiH groups were found in the structure of SiO_2 glass with SiOH groups and H_2 molecules by reaction between H_2 and SiO_2 glass (Schmidt et al., 1998). The report described that the SiH vibration mode of SiO_2 glass appeared at around 2250 cm^{-1} after quenching from 0.2 GPa and around 1100 K to 1300 K to ambient condition (Schmidt et al., 1998). The SiH frequency in the SiO_2 glass is markedly higher than that observed in the present study (2188 cm^{-1} at 0.4 GPa, see Figure 2b). Solid silane (SiH_4), which is the simplest molecule that contains SiH groups, exhibits the SiH vibration mode at 2190 cm^{-1} at 1.7 GPa (Chen et al., 2008), which is substantially lower than the SiH vibration mode observed in the present study. In case of SiH_4 coexisting with H_2, a miscible fluid phase was formed up to around 6 GPa at room temperature (Wang et al., 2009). The SiH vibration mode of the SiH_4-H_2 fluid shifted to higher frequencies compared with that of pure silane, and the SiH vibration frequency increases concomitantly with increasing H_2/SiH_4 ratio (Wang et al., 2009) (see Fig. 2b). The higher SiH vibration frequency than that of the pure SiH_4 was explainable by intermolecular interaction between the SiH_4 and surrounding H_2 fluid (Wang et al., 2009). The present SiH frequency appeared even higher than that observed by Wang et al. (2009) in the SiH_4-H_2 fluid with the H_2/SiH_4 of

192 5. Results obtained in the present study suggest the formation of a SiH_4-H_2 miscible
193 fluid with H_2/SiH_4 greater than 5. SiH_4 molecules are likely to be formed with a
194 chemical reaction between dissolved SiO_2 components and H_2 fluid. For SiH_4-H_2 fluid,
195 downshifting of the stretching mode of H_2 molecules was reported (Wang et al., 2009),
196 although no such a shift was observed in the present study (Fig. 1b). The H_2/SiH_4 ratio
197 in the present study is considerably higher than that observed in the previous SiH_4-H_2
198 experiment (Wang et al., 2009), and downshift of the HH stretching mode is regarded as
199 too small to be detected.

200 The OH stretch frequency with decreasing pressure from 3.0 GPa to 2.1 GPa
201 observed in this study correspond to that of ice VII, even though the OH vibration mode
202 of this study was obtained from the IR absorption spectra and that of ice VII was
203 measured using Raman spectra (Walrafen et al., 1982) (Fig. 4b). At 1.4 GPa and 1.1
204 GPa, the OH vibration frequency corresponds to that of ice VI measured using Raman
205 spectroscopy (Abebe and Walrafen, 1979). Additionally, the phase transition pressure
206 between ice VI and ice VII was reported at around 2 GPa, room temperature (Pistoriu et
207 al., 1968), which is approximately consistent with the pressure of the jump of OH
208 vibration mode observed in the present study. These facts indicate that the OH vibration

mode observed in this study originated from H_2O molecules. Molar concentration of H_2O in the fluid phase was estimated roughly as 1 % using molar absorptivity for the OH stretching mode of liquid water (81 liter mol^{-1} cm^{-1}) (Thompson, 1965).

Results of the present study suggest the formation of SiH_4 and H_2O by the dissolution of quartz in H_2, indicating the chemical reaction between dissolved SiO_2 components and solvent H_2. In this case, direct bonding between H atoms and a Si atom was formed. By dissolution of SiO_2 composition in H_2O fluid, SiOH groups such as H_4SiO_4 and/or its polymer were observed at high-pressure and high-temperature conditions between about 500 and 800 cm^{-1} in Raman spectra (Zotov and Keppler, 2000; Zotov and Keppler, 2002; Mysen, 2009; Mysen, 2010). The SiOH group and CH_3 group were also found by reaction of SiO_2 and CH_4 fluid in a reduced condition where CH_4 is the most abundant C-O-H fluid with H_2O fluid and minor amount of H_2 fluid (Mysen and Yamashita, 2010). In these cases, Si-H groups formation was not reported. The dissolution species in H_2 fluid differs greatly from those observed in H_2O and CH_4 fluids. The new chemical reaction with the dissolution observed in this study might be related to the high solubility of the SiO_2 composition in H_2 fluid.

Implications

The ratio of H_2/H_2O in the mantle was regarded as controlled by the surrounding oxidation states (e.g. Ballhaus and Frost, 1994; Ballhaus, 1995; Frost and McCammon, 2008; Sokol et al., 2009), i.e., the oxidation of H_2 to H_2O is induced by the reduction of iron contained in silicate minerals. However, results of the present study showed the formation of H_2O molecules by the chemical reaction between SiO_2 and H_2 fluid in an iron-free system. We inferred that a part of H_2 in the mantle oxidized to form H_2O with dissolution or melting of coexisting silicate minerals. The ratio of H_2/H_2O in the mantle might depend not only on surrounding $Fe^{3+}/\sum Fe$, but also on the dissolution and melting of SiO_2 components. To ascertain the ratio of H_2/H_2O in the fluid in the mantle, additional experiments should be conducted in more realistic mantle compositions, in which not only $Fe^{3+}/\sum Fe$, but also the phase relation and melting of silicate minerals should be involved.

Acknowledgments

This study was supported by the G-COE program Deep Earth Mineralogy and the Sasakawa Scientific Research Grant from The Japan Science Society. A. Shinozaki was supported by a JSPS Research Fellowship for Young Scientists. This study was conducted under the Visiting Researcher's Program of the Institute for Solid State Physics,

243 The University of Tokyo. Synchrotron radiation experiments were performed at BL43IR
244 of SPring-8, Japan, with the approval of the Japan Synchrotron Radiation Research
245 Institute (JASRI) (Proposal No. 2012B1104). We thank Dr. T. Moriwaki for supporting
246 the FT-IR measurements at BL43IR, SPring-8.

247

References

Abebe, M., and Walrafen, G.E. (1979) Raman studies of ice-VI using a diamond anvil cell. Journal of Chemical Physics, 71(10), 4167-4169.

Anderson, G.M., and Burnham, C.W. (1965) Solubility of quartz in supercritical water American Journal of Science, 263(6), 494-&.

Bali, E., Audétat, A., and Keppler, H. (2013) Water and hydrogen are immiscible in Earth's mantle. Nature, 495(7440), 220-222.

Ballhaus, C. (1995) Is the upper mantle metal-saturated? Earth and Planetary Science Letters, 132(1-4), 75-86.

Ballhaus, C., and Frost, B.R. (1994) The generation of oxidized CO_2-bearing basaltic melts from reduced CH_4-bearing upper mantle sources. Geochimica et Cosmochimica Acta, 58(22), 4931-4940.

Chen, X.J., Struzhkin, V.V., Song, Y., Goncharov, A.F., Ahart, M., Liu, Z.X., Mao, H., and Hemley, R.J. (2008) Pressure-induced metallization of silane. Proceedings of the National Academy of Sciences of the United States of America, 105(1), 20-23.

Dean, K.J., Sherman, W.F., and Wilkinson, G.R. (1982) Temperature and

pressure-dependence of the Raman active-mode of vibration of α-quartz. Spectrochimica Acta Part A - Molecular and Biomolecular Spectroscopy, 38(10), 1105-1108.

Frost, D.J., and McCammon, C.A. (2008) The redox state of Earth's mantle. Annu. Rev. Earth Planet. Sci., 36, 389-420.

Goncharov, A.G., Ionov, D.A., Doucet, L.S., and Pokhilenko, L.N. (2012) Thermal state, oxygen fugacity and C-O-H fluid speciation in cratonic lithospheric mantle: New data on peridotite xenoliths from the Udachnaya kimberlite, Siberia. Earth and Planetary Science Letters, 357, 99-110.

Gush, H.P., Hare, W.F.J., Allin, E.J., and Welsh, H.L. (1960) The infrared fundamental band of liquid and solid hydrogen Canadian Journal of Physics, 38(2), 176-193.

Hashimoto, G.L., Abe, Y., and Sugita, S. (2007) The chemical composition of the early terrestrial atmosphere: Formation of a reducing atmosphere from CI-like material. Journal of Geophysical Research-Planets, 112 (E5).

Hirschmann, M.M., Withers, A.C., Ardia, P., and Foley, N.T. (2012) Solubility of molecular hydrogen in silicate melts and consequences for volatile evolution of terrestrial planets. Earth and Planetary Science Letters, 345, 38-48.

Inoue, T. (1994) Effect of water on melting phase relations and melt composition in the system Mg_2SiO_4-$MgSiO_3$-H_2O up to 15 GPa. Physics of the Earth and Planetary Interiors, 85(3-4), 237-263.

Katz, A.I., Schiferl, D., and Mills, R.L. (1984) New Phases and chemical-reactions in solid CO under pressure. Journal of Physical Chemistry, 88(15), 3176-3179.

Kawamoto, T., Matsukage, K.N., Mibe, K., Isshiki, M., Nishimura, K., Ishimatsu, N., and Ono, S. (2004) Mg/Si ratios of aqueous fluids coexisting with forsterite and enstatite based on the phase relations in the Mg_2SiO_4-SiO_2-H_2O system. American Mineralogist, 89(10), 1433-1437.

Manning, C.E. (1994) The solubility of quartz in H_2O in the lower crust and upper mantle. Geochimica et Cosmochimica Acta, 58(22), 4831-4839.

Mao, H., Bell, P., Shaner, J.W., and Steinberg, D. (1978) Specific volume measurements of Cu, Mo, Pd, and Ag and calibration of the ruby R_1 fluorescence pressure gauge from 0.06 to 1 Mbar. Journal of Applied Physics, 49(6), 3276-3283.

McCammon, C., and Kopylova, M.G. (2004) A redox profile of the slave mantle and oxygen fugacity control in the cratonic mantle. Contributions to Mineralogy and Petrology, 148(1), 55-68.

299 Mibe, K., Fujii, T., and Yasuda, A. (2002) Composition of aqueous fluid coexisting with
300 mantle minerals at high pressure and its bearing on the differentiation of the
301 Earth's mantle. Geochimica et Cosmochimica Acta, 66(12), 2273-2285.
302 Mysen, B.O. (2009) Solution mechanisms of silicate in aqueous fluid and H_2O in
303 coexisting silicate melts determined in-situ at high pressure and high
304 temperature. Geochimica et Cosmochimica Acta, 73(19), 5748-5763.
305 Mysen, B. O. (2010) Speciation and mixing behavior of silica-saturated aqueous fluid at
306 high temperature and pressure. American Mineralogist, 95(11-12), 1807-1816.
307 Mysen, B.O., and Yamashita, S. (2010) Speciation of reduced C-O-H volatiles in
308 coexisting fluids and silicate melts determined in-situ to similar to ~1.4 GPa and
309 800°C. Geochimica et Cosmochimica Acta, 74(15), 4577-4588.
310 Newton, R.C., and Manning, C.E. (2003) Activity coefficient and polymerization of
311 aqueous silica at 800 degrees°C, 12 kbar, from solubility measurements of
312 SiO_2-buffering mineral assemblages. Contributions to Mineralogy and Petrology,
313 146(2), 135-143.
314 Newton, R.C., and Manning, C.E. (2008) Thermodynamics of SiO_2-H_2O fluid near the
315 upper critical end point from quartz solubility measurements at 10 kbar. Earth

316 and Planetary Science Letters, 274(1-2), 241-249.

317 Pistoriu, C.W.F.T., Rapoport, E., and Clark, J.B. (1968) Phase diagrams of H_2O and

318 D_2O at high pressures. Journal of Chemical Physics, 48(12), 5509-5514.

319 Rohrbach, A., Ballhaus, C., Golla-Schindler, U., Ulmer, P., Kamenetsky, V.S., and

320 Kuzmin, D.V. (2007) Metal saturation in the upper mantle. Nature, 449(7161),

321 456-8.

322 Schaefer, L., and Fegley, B. (2007) Outgassing of ordinary chondritic material and some

323 of its implications for the chemistry of asteroids, planets, and satellites. Icarus,

324 186(2), 462-483.

325 Schmidt, B.C., Holtz, F.M., and Beny, J.M. (1998) Incorporation of H_2 in vitreous silica,

326 qualitative and quantitative determination from Raman and infrared

327 spectroscopy. Journal of Non-Crystalline Solids, 240(1-3), 91-103.

328 Schmidt, C., and Ziemann, M.A. (2000) In-situ Raman spectroscopy of quartz: A

329 pressure sensor for hydrothermal diamond-anvil cell experiments at elevated

330 temperatures. American Mineralogist, 85(11-12), 1725-1734.

331 Sharma, S., Mao, H., and Bell, P. (1980) Raman measurements of hydrogen in the

332 pressure range 0.2-630 kbar at room temperature. Physical Review Letters,

44(13), 886-888.

Shen, A., and Keppler, H. (1995) Infrared spectroscopy of hydrous silicate melts to 1000 degrees°C and 10 kbar: Direct observation of H_2O speciation in a diamond-anvil cell. American Mineralogist, 80(11-12), 1335-1338.

Shinozaki, A., Hirai, H., Ohfuji, H., Okada, T., Machida, S., and Yagi, T. (2013) Influence of H_2 fluid on the stability and dissolution of Mg_2SiO_4 forsterite under high pressure and high temperature. American Mineralogist, 98, 1604-1609.

Sleep, N.H., Meibom, A., Fridriksson, T., Coleman, R.G., and Bird, D.K. (2004) H_2-rich fluids from serpentinization: Geochemical and biotic implications. Proceedings of the National Academy of Sciences of the United States of America, 101(35), 12818-12823.

Sokol, A.G., Palyanova, G.A., Palyanov, Y.N., Tomilenko, A.A., and Melenevsky, V.N. (2009) Fluid regime and diamond formation in the reduced mantle: Experimental constraints. Geochimica et Cosmochimica Acta, 73(19), 5820-5834.

Stalder, R., Ulmer, P., Thompson, A., and Günther, D. (2001) High pressure fluids in the system $MgO-SiO_2-H_2O$ under upper mantle conditions. Contributions to

Mineralogy and Petrology, 140(5), 607-618.

Takemura, K., Ch., S.P., Kunii, Y., and Toma, Y. (2001) Versatile gas-loading system for diamond-anvil cells. Review of Scientific Instruments, 72(10), 3873-3876.

Thompson, W.K. (1965) Infra-red spectroscopic studies of aqueous systems. 1. Transactions of the Faraday Society, 61(516), 1635-1640.

Walrafen, G.E., Abebe, M., Mauer, F.A., Block, S., Piermarini, G.J., and Munro, R. (1982) Raman and X-ray investigations of Ice VII to 36.0 GPa. Journal of Chemical Physics, 77(4), 2166-2174.

Wang, S., Mao, H.K., Chen, X.J., and Mao, W.L. (2009) High pressure chemistry in the H_2-SiH_4 system. Proceedings of the National Academy of Sciences of the United States of America, 106(35), 14763-14767.

Wood, B.J., Bryndzia, L.T., and Johnson, K.E. (1990) Mantle oxidation-state and its relationship to tectonic environment and fluid speciation. Science, 248(4953), 337-345.

Woodland, A.B., and Koch, M. (2003) Variation in oxygen fugacity with depth in the upper mantle beneath the Kaapvaal craton, southern Africa. Earth and Planetary Science Letters, 214(1-2), 295-310.

Yagi, T., Yusa, H., and Yamakata, M. (1996) An apparatus to load gaseous materials to the diamond-anvil cell. Review of Scientific Instruments, 67(8), 2981-2984.

Yamada, A., Inoue, T., Urakawa, S., Funakoshi, K.I., Funamori, N., Kikegawa, T., and Irifune, T. (2011) In situ X-ray diffraction study on pressure-induced structural changes in hydrous forsterite and enstatite melts. Earth and Planetary Science Letters, 308(1-2), 115-123.

Zhang, Y.G., and Frantz, J.D. (2000) Enstatite-forsterite-water equilibria at elevated temperatures and pressures. American Mineralogist, 85(7-8), 918-925.

Zotov, N., and Keppler, H. (2000) In-situ Raman spectra of dissolved silica species in aqueous fluids to 900 °C and 14 kbar. American Mineralogist, 85(3-4), 600-603.

Zotov, N., and Keppler, H. (2002) Silica speciation in aqueous fluids at high pressures and high temperatures. Chemical Geology, 184(1-2), 71-82.

382 **Figure legends**

383 Fig. 1 Representative Raman spectra of fluid + quartz at 1.7 GPa before heating and
384 fluid phase at 2.0 GPa after heating in two Raman shift regions: (a) between 200 cm^{-1}
385 and 800 cm^{-1} and (b) between 4100 cm^{-1} to 4300 cm^{-1}.

386 Fig. 2 (a) Raman spectra of a SiH vibration mode obtained from the fluid phase after
387 heating with decreasing pressure in the region from 2100 cm^{-1} to 2300 cm^{-1}. A broad
388 peak at around 2200 cm^{-1} is the secondary peak of diamond used as anvils. (b) Pressure
389 dependence of frequencies of the SiH vibration modes.

390 Fig. 3 Optical microphotograph of the sample after heating at 1500 K, 3.0 GPa. A square
391 in the picture shows the measured area of the IR spectra (15 μm × 15 μm).

392 Fig. 4(a) Representative IR absorption spectra with decreasing pressure at room
393 temperature between 2700 cm^{-1} to 5200 cm^{-1}. (b) Pressure dependence of the frequencies
394 of OH vibration modes. Those of ice VI and ice VII were referred from earlier reports
395 (Abebe and Walrafen, 1979; Walrafen et al., 1982).

This is a preprint, the final version is subject to change, of the American Mineralogist (MSA)
Cite as Authors (Year) Title. American Mineralogist, in press.
(DOI will not work until issue is live.) DOI: http://dx.doi.org/10.2138/am.2014.4798

Fig. 1a

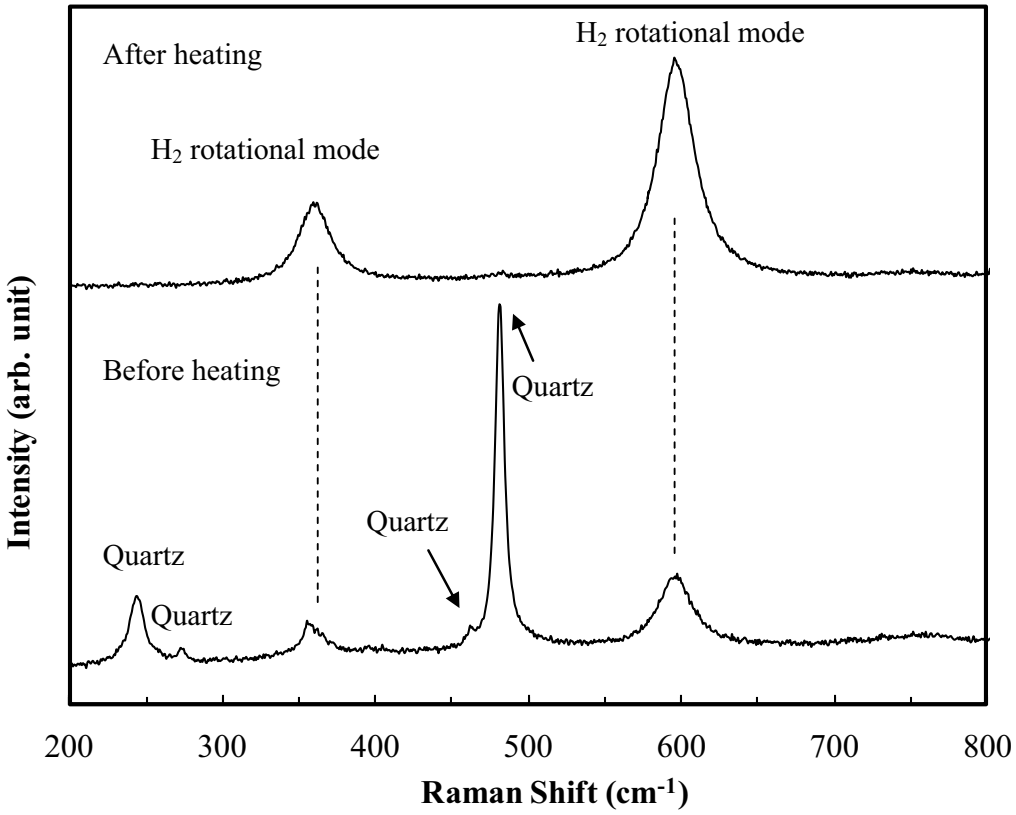

Fig. 1b

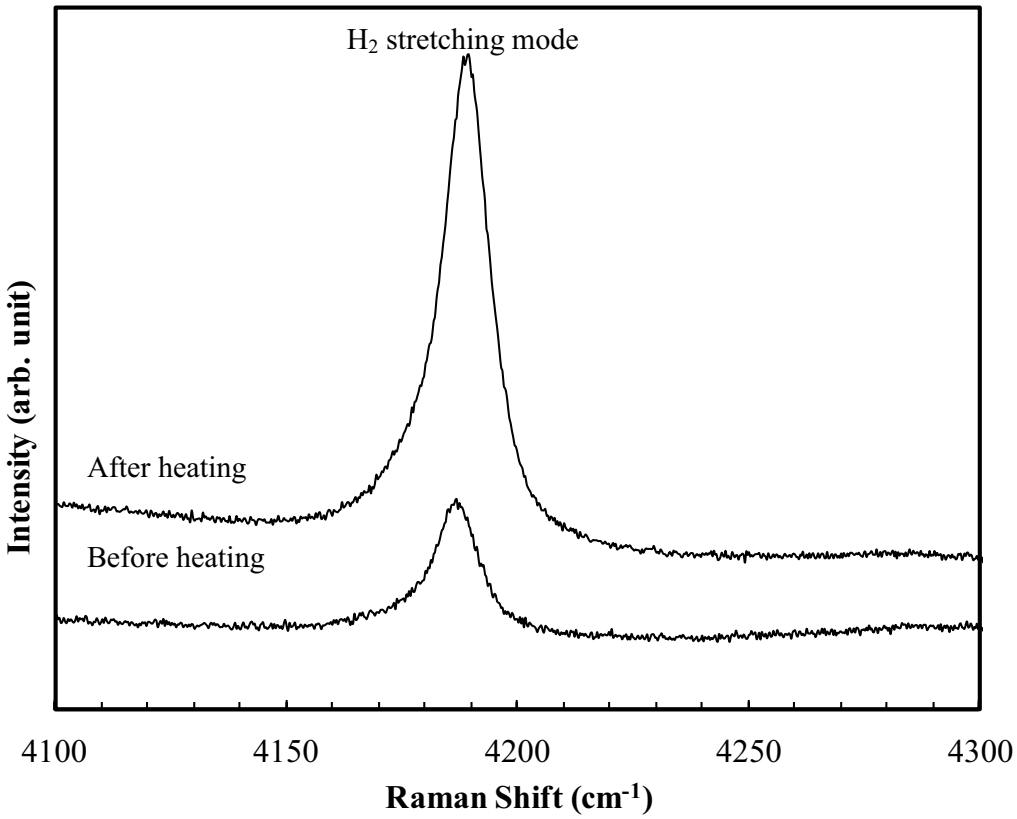
H2 stretching mode
After heating
Before heating
Intensity (arb. unit)
4100
4150
4200
4250
4300
Raman Shift (cm-1)

Fig. 2a

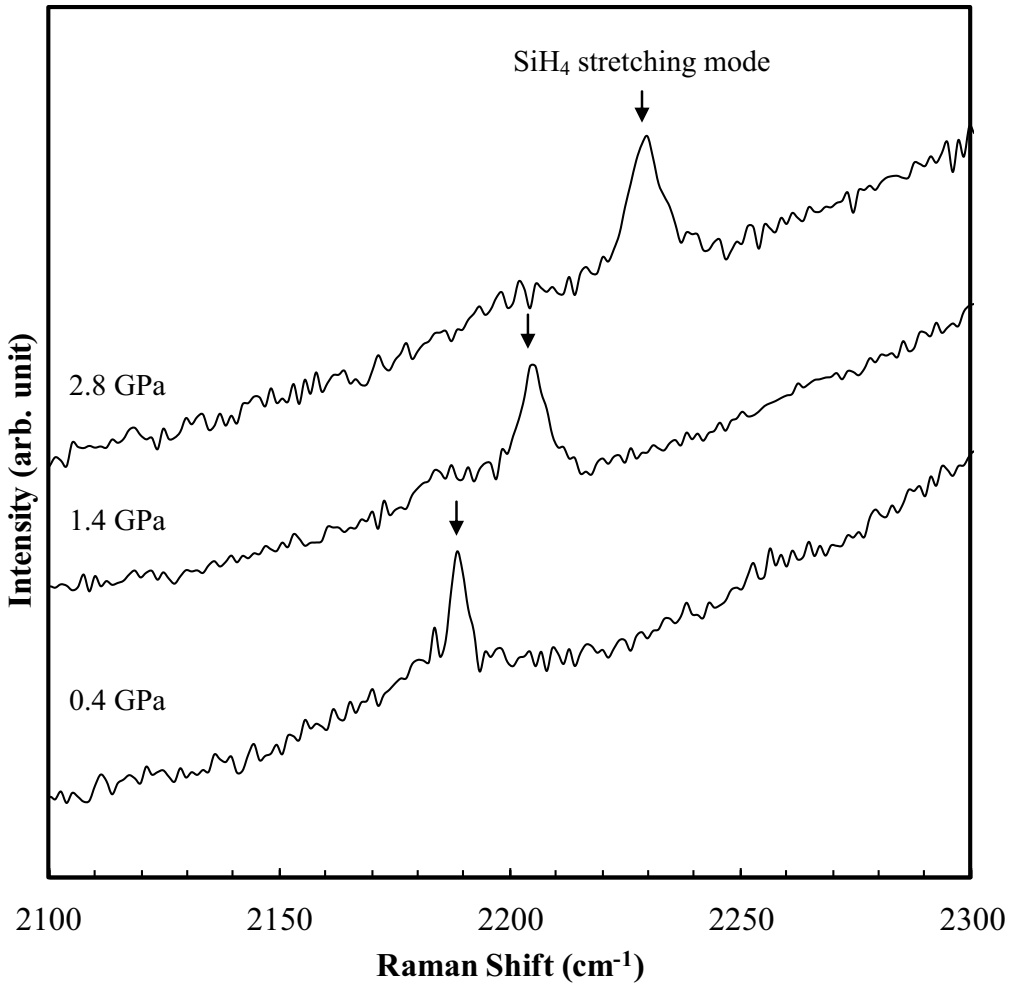
SiH4 stretching mode
2.8 GPa
1.4 GPa
0.4 GPa
Intensity (arb. unit)
2100
2150
2200
2250
2300
Raman Shift (cm-1)

Fig. 2b

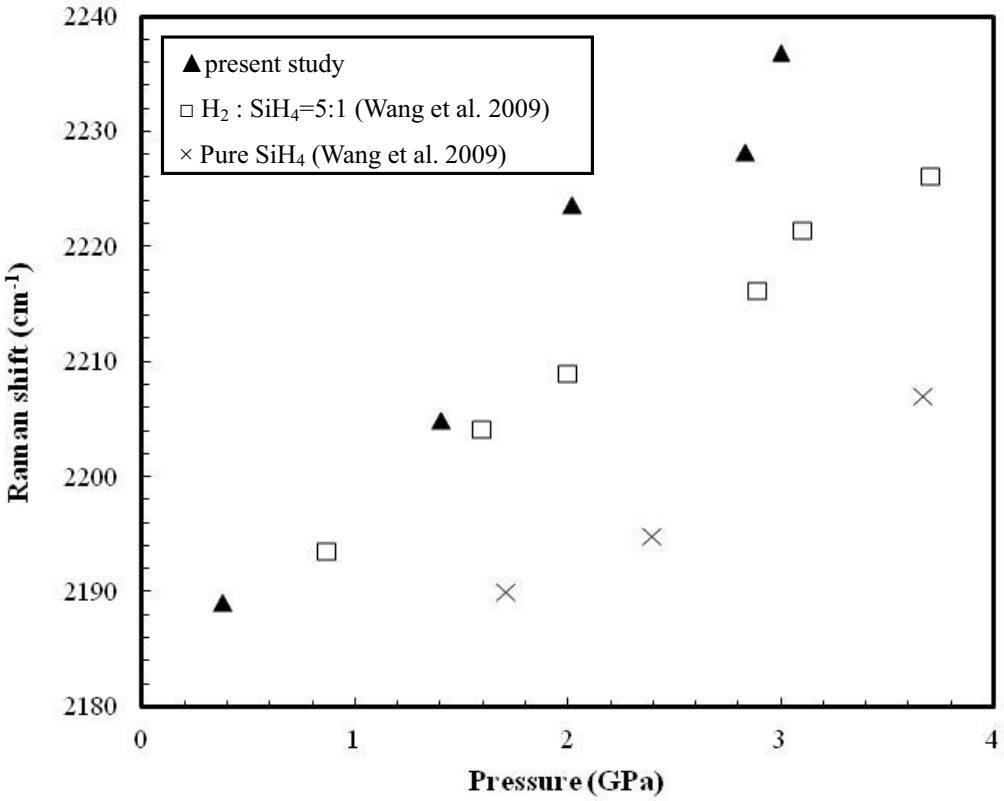
▲present study
□ H_2 : SiH_4=5:1 (Wang et al. 2009)
× Pure SiH_4 (Wang et al. 2009)
Raman shift (cm^{-1})
Pressure (GPa)
2240
2230
2220
2210
2200
2190
2180
0
1
2
3
4

Fig. 3

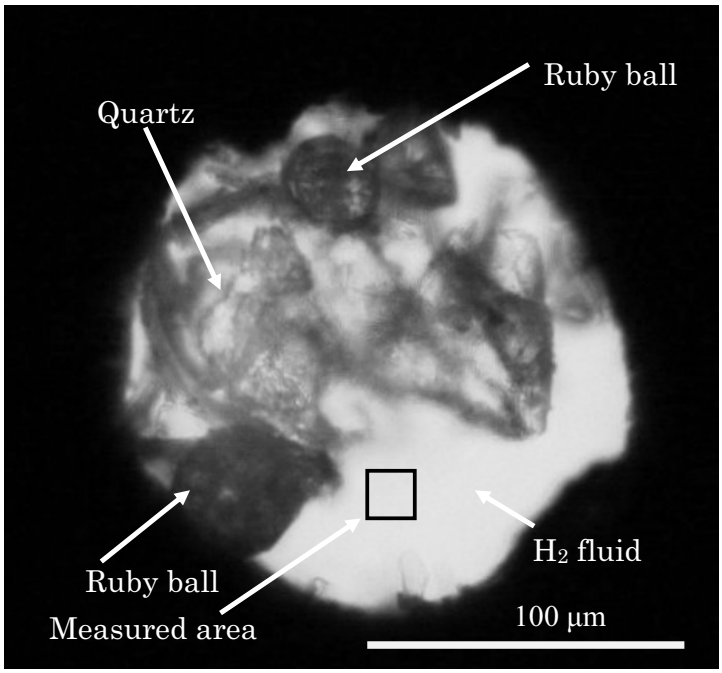

Fig. 4a

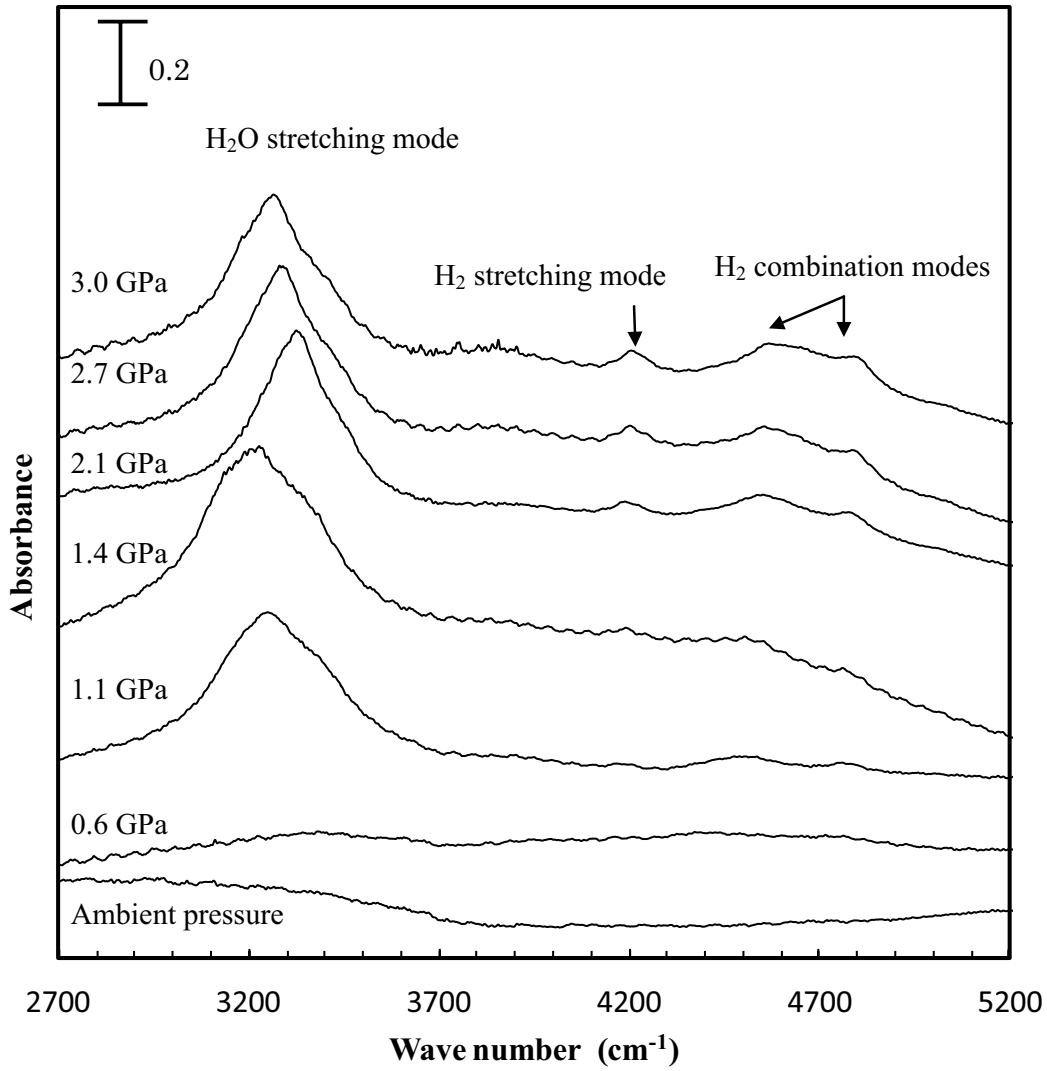
0.2
H2O stretching mode
H2 stretching mode
H2 combination modes
3.0 GPa
2.7 GPa
2.1 GPa
1.4 GPa
1.1 GPa
0.6 GPa
Ambient pressure
Absorbance
2700
3200
3700
4200
4700
5200
Wave number (cm-1)

Fig. 4b

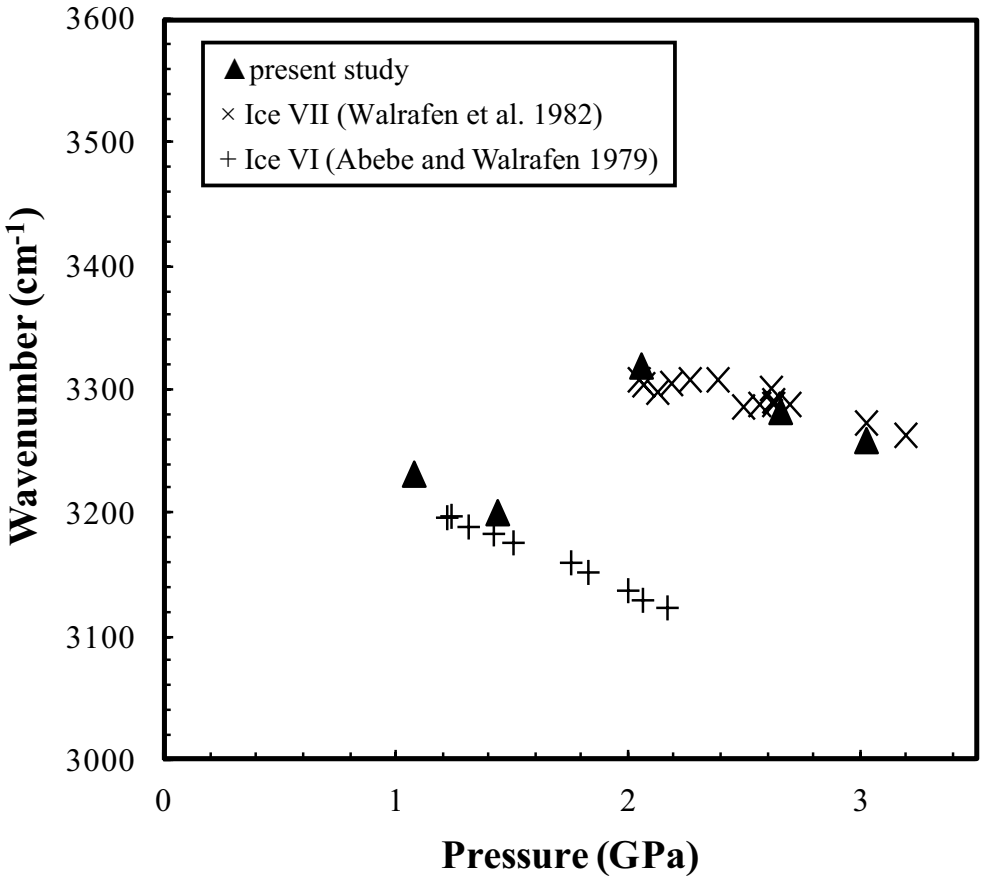
▲present study
× Ice VII (Walrafen et al. 1982)
+ Ice VI (Abebe and Walrafen 1979)
Wavenumber (cm-1)
3600
3500
3400
3300
3200
3100
3000
0
1
2
3
Pressure (GPa)